Planta (2008) 228:851–862
DOI 10.1007/s00425-008-0787-0

ORIGINAL ARTICLE

ScORK17, a transmembrane receptor-like kinase predominantly expressed in ovules is involved in seed development

Hugo Germain · Madoka Gray-Mitsumune · Edith Lafleur · Daniel P. Matton

Received: 4 June 2008 / Accepted: 4 July 2008 / Published online: 23 July 2008

Abstract The mRNA expression of the *Solanum chacoense* Ovule Receptor Kinase 17 (ScORK17), a receptor kinase of the LRR-VI subfamily, is highly specific to the female reproductive tissues. No LRR-VI subfamily members in any plant species have yet been attributed a function. A phylogenetic tree inferred using the kinase domain of LRR-VI subfamily members separated the family into two clades: one containing an average of 8.2 LRR per protein and a second clade containing an average of 2.7. In situ hybridization analyses showed that the *ScORK17* signal was mainly detected in the single ovule integument and in the endothelium. Transient expression analysis also revealed that *ScORK17* was N-glycosylated in planta. Overexpression of *ScORK17* in *S. chacoense* did not produce plants with an altered phenotype. However, when heterologous transformation was performed with a full-length *ScORK17* clone in *A. thaliana*, the resulting transgenic plants showed reduced seed set, mainly due to aberrant embryo sac development, thus supporting a developmental role for *ScORK17* in ovule and seed development.

Keywords Plant receptor kinase · Heterologous transformation · Ovule development · Seed set

Genbank accession number: EF517229.

Hugo Germain and Madoka Gray-Mitsumune are the two authors who contributed equally to this manuscript.

H. Germain · M. Gray-Mitsumune · E. Lafleur · D. P. Matton (✉)
Département de Sciences Biologiques,
Institut de Recherche en Biologie Végétale (IRBV),
Université de Montréal, 4101 Sherbrooke est,
Montréal, QC H1X 2B2, Canada
e-mail: dp.matton@umontreal.ca

Introduction

Complex organisms, such as plants, use elaborate communication schemes between cells in order to ensure optimal growth and development. Receptor kinases are well suited as mediators of this intercellular communication mechanism. Their extracellular domain can perceive the information (ligand) coming from the environment or from neighboring cells and relay this information to the nucleus via the phosphorylation of intracellular protein targets through the action of their intracellular kinase domain. During the last decade receptor-like kinases (RLKs) have been associated with nearly all aspects of plant growth and development, including pathogen perception (Gomez-Gomez and Boller 2000), hormone signaling (Li and Chory 1997; Matsubayashi et al. 2002), anther and embryo development (Canales et al. 2002), organ initiation (Torii et al. 1996), and meristem maintenance (Clark et al. 1993, 1997).

Despite all the functions accomplished by receptor kinases, few RLK have been associated with seed development. *EXTRA SPOROGENOUS CELLS* (*EXS*) and *CRINKLY4* are two RLKs for which mutants were found to be impaired in seed development. *EXS* mutant plants accumulate a larger number of sporogenous cells in the anther and have smaller embryonic cells, delayed embryo development, and smaller mature embryos (Canales et al. 2002). *CRINKLY4* was discovered in maize (Becraft et al. 1996), where loss of *CRINKLY4* function inhibits aleurone formation in the seed and affects leaf epidermal cell differentiation (Becraft et al. 1996). *CRINKLY4* was also characterized in *Arabidopsis* (*ACR4*) where it was shown that overexpression or antisense suppression of *ACR4* lead to embryo malformation (Tanaka et al. 2002) and also disrupted cell layer organization of epidermis-related tissues in leaf and during ovule integument development (Gifford

et al. 2003; Watanabe et al. 2004). The *SUB* RLK was also originally isolated on the basis of its role in ovule outer integument development (Chevalier et al. 2005). More recently, it was shown that disruption of the *TOADSTOOL2* and *RPK1* genes result in a loss of radial patterning and basal pole defects during early embryogenesis (Nodine et al. 2007). Also related to protoderm specification, the *ALE2* RLK was shown to function in the same genetic process as *ACR4* (Tanaka et al. 2007). Finally, the *FERONIA* (*FER*) gene was shown to code for a RLK involved in the female control of pollen tube reception. In *feronia* plants, the pollen tube fails to arrest and continues to grow inside the female gametophyte, thus impairing fertilization (Escobar-Restrepo et al. 2007).

Apart from gain of function and loss of function mutants, heterologous transformation can also be highly informative when trying to assign a function to a gene. Heterologous transformation has generally been used to evaluate the functional equivalence or relationship between related genes of different species (Chantha et al. 2006). Several studies in plants have reported the use of heterologous transformation in order to evaluate the role of gene in other species when no phenotype was observed in the host species or when functional redundancy among members of gene families hampers the use of loss-of-function or knockout lines (Fu et al. 2007; Hirschi 1999; Hirschi et al. 2000). For example, membrane transporter protein originating from multigene family, such as permease, H^+-ATPase, and cyclic nucleotide-gated cation channel, have been transformed in yeast in order to study the effect and specificity of individual genes (Alemzadeh et al. 2006; Ali et al. 2006; Weig and Jakob 2000). Heterologous transformation has also been used from one plant species to another. For example, the *CAX1* and *CAX2* genes (*calcium exchanger 1* and *2*) are functionally redundant in *Arabidopsis* and loss-of-function mutant of either gene do not display a detectable phenotype in *Arabidopsis* (Hirschi et al. 2000). Additionally, plants overexpressing the *CAX2* gene in *Arabidopsis* do not show an altered protein level of CAX2, but when the *AtCAX2* is overexpressed in tobacco, the transgenic plants accumulate higher levels of Ca^{2+}, Cd^{2+}, and Mn^{2+}, and were more tolerant to elevated Mn^{2+} levels (Hirschi et al. 2000). Other examples of plant/plant heterologous transformation revealing gene function is the expression of the *Solanum tuberosum* MADS-box gene *StMADS16* in tobacco (Garcia-Maroto et al. 2000) and the successful expression of the barley *HVA1* gene in the perennial grass *Agrostis stolonifera* that resulted in increased tolerance to water-deficit stress in this species (Fu et al. 2007).

From a subtraction screen that focused on weakly expressed transcripts in ovule and ovary tissues following fertilization, we have isolated 30 receptor-like kinase genes named *ScORK1* to *30* for *Solanum chacoense* Ovule Receptor Kinase (Germain et al. 2005). Detailed expression analysis through quantitative RT-PCR showed that amongst the 30 RLKs, 28 were predominantly expressed in female reproductive tissues and 23 were transcriptionally up-regulated following fertilization. Of these, four (*ScORK2*, *ScORK17*, *ScORK18*, and *ScORK24*) were members of the LRR-VI family. In this paper we have used expression analysis and heterologous transformation in order to decipher the possible roles of *ScORK17*. Expression of *ScORK17* in *Arabidopsis thaliana* lead to incomplete seed set resulting from abnormal embryo sac development. To our knowledge this is the first report of a potential function for a member of the LRR-VI subfamily of receptor-like kinases.

Materials and methods

Sequence analysis

Raw DNA sequence was in silico translated using MacVector 8.1.2 (Accelrys, San Diego, CA, USA). The presence of a signal peptide was assessed using SignalP 3.0 (Bendtsen et al. 2004) and the location of the transmembrane domain was positioned using TMHMM 2.0 (Krogh et al. 2001). Putative N-glycosylation sites were analyzed using NetNGly 1.0 (Gupta and Brunak 2002) and the structure of the leucine-rich repeat domain was analyzed using ScanSite 2.0 (Obenauer et al. 2003). The phylogenic tree was inferred using a neighbor-joining algorithm (Saitou and Nei 1987) with 10,000 bootstraps either on the full length sequences or on the trimmed catalytic domains.

Transgenic plants production and analysis

S. chacoense transgenics were either overexpression lines (OX) with the full length *ScORK17* cDNA cloned downstream of the CaMV 35S promoter or truncated *ScORK17* expressing only the signal peptide, extracellular domain and transmembrane domain (dominant negative construct) cloned downstream of the CaMV 35S promoter. Prior to transformation all constructs were fully sequenced. *S. chacoense* transformation with *Agrobacterium tumefaciens* strain LBA4404 was carried out as described previously (Matton et al. 1997). Transgenic *Arabidopsis* plants consisted either of the GABI-Kat 055D10 insertional mutant line for At3g03770 (Rosso et al. 2003) or lines that have been agroinfiltrated with the above mentioned *S. chacoense* constructs. *A. thaliana* Col-0 plants were grown under long day conditions (16 h light/8 h dark) at 25°C in a growth chamber in 1:1:1 mixture of perlite, vermiculite and topsoil. *S. chacoense* plants were greenhouse grown in topsoil.

Seed count and clearing

Siliques were harvested and placed in deionized water. Dehydration was performed by transferring the siliques in increasing concentration solutions of ethanol (25, 50, 75, 100%) for 1 h each and placed in a fresh 100% ethanol solution overnight. For clearing with methylsalicylate, the siliques were transferred in increasing ratio of methylsalicylate/ethanol solutions (25:75, 50:50, 75:25, 100:0) for 1 h each and left overnight in 100% methylsalicylate. The number of seeds per siliques was counted under a stereomicroscope and observed at a magnification of 10×. Cleared silique photographs were taken on a Zeiss Discovery V12 stereomicroscope while for DIC microscopy, cleared ovules were observed at a magnification of 63× on a Zeiss M1 Axioimager. Pictures were taken with a Zeiss Axiocam HRc camera.

RNA expression analyses

RNA for RT-PCR analysis and RNA gel blot analysis was isolated using the RNeasy® plant mini kit (Qiagen, Mississauga, ON, Canada). The RNA concentration was determined by measuring its absorbance at 260 nm and verified by agarose gel electrophoresis and ethidium bromide staining. Equal loading of total RNA on RNA gel blots was verified with a *S. chacoense* 18S RNA probe. RNA gel blot analyses were performed as described previously (O'Brien et al. 2002). Probe for RNA blot were synthesized using a random-labeled PCR kit (Ambion, Austin, TX, USA). Membranes were exposed at room temperature on a europium screen and scanned on a Typhoon 9200 Phosphorimager (GE Healthcare, Baie d'Urfé, QC, Canada). In situ hybridizations were performed as described previously (Gray-Mitsumune et al. 2006; O'Brien et al. 2005). Microscopic observations were made on a Zeiss Axioimager M1 microscope and pictures were taken with a Zeiss Axiocam HRc camera. For RT-PCR, amplification conditions were as previously described (Germain et al. 2005). The amplification was stopped after 31 cycles and the gel was stained using ethidium bromide. Actin was used as a control (forward primer ATAACCATCGGAGCCTGAGAGATTCC reverse primer TTGAAATCCACATCTGTTGGAAGGT).

Transient expression for protein localization

The *ScORK17* open reading frame was introduced by recombination in the Gateway pZeo donor vector (Invitrogen, Burlington, ON, Canada). From the donor vector, the *ScORK17* open reading frame was transferred by recombination in the pMDC83 vector (Curtis and Grossniklaus 2003). Onion cells were transiently transformed by particle bombardment using this *ScORK17-GFP-6×His* construct. A total of 5 µg of DNA was mixed with 10 µl of 0.1 M spermidine, 25 µl of 2.5 M $CaCl_2$ and 25 µl of tungsten microcarrier (60 µg/ml in 50% glycerol), vortexed vigorously for 5 min and centrifuged at 800*g* in a microcentrifuge for 10 s. The pellet was washed once with 70% ethanol and was resuspended in 5 µl 100% ethanol. The DNA-tungsten particles were bombarded into cells at a pressure of 1,200 psi and target distance of 10 cm, with a homemade biolistic/He particle delivery system under a vacuum chamber at a pressure of 24 mm Hg. The transformed cells were kept alive by placing the onion peels onto 0.5× Murashige-Skoog medium overnight.

Deglycosylation assay

For N-deglycosylation assay, the *ScORK17* construct used for protein localization was expressed in planta through agroinfiltration of *Nicotiana benthamiana* leaves co-infected with the p19 silencing suppressor gene as previously described (Voinnet et al. 2003). Crude extracts from infected leaves collected 3 days after infection were treated with N-glycosidase F (PNGase F) following the manufacturer's instructions (New England Bio-lab, Pickering, ON, Canada). The extract was separated on acrylamide gel, transferred on PVDF membrane and detected using the anti-HIS antibody (Sigma, Oakville, ON, Canada).

Immunoblotting procedure

The SDS-PAGE gel was run at 150 V for 1 h in running buffer (1 g SDS, 3.03 g Tris and 14.41 g glycine in 1 L) and then transferred to PVDF membrane in transfer buffer (3.03 g Tris and 14.41 g glycine and 200 mL methanol in 1 L). Immunoblotting was done as follows: PVDF membranes were hydrated in methanol for 10 s, equilibrated in TBS (20 mM Tris pH7,5, 150 mM NaCl) for 15 min, blocked for 1 h in TBST + Milk (TBS + 0.02% Tween 20 and 2.5% defatted dry-milk), incubated for 1 h with the anti-His antibody in TBST + Milk, washed three times in TBST (15 min each), incubated with the monoclonal anti-rabbit IgG γ-chain specific antibody conjugated with the peroxidase (Sigma) for 1 h and washed three times 15 min in TBST. Detection was done using ECL Plus (GE Healthcare, Baie d'Urfé, QC, Canada) and exposed on a Bioflex Econo Film (Interscience, Laval, Qc, Canada).

Results

ScORK17 sequence analysis and phylogeny

The EST corresponding to *ScORK17* (DN980445) was fully sequenced and most probably contained the full-

length or near full-length *ScORK17* cDNA (2,665 bp, Genbank accession number EF517229) since it corresponded to the length obtained by RNA gel blot analysis (~2,600 nt, see Fig. 2). The longest open reading frame deduced from the cDNA sequence coded for an 85.8 kD protein of 778 amino acids with a predicted pI of 8.42. The first methionine found is located at position 53 of the longest translated product (nucleotide position 159–161). Although no in frame stop codon was found upstream of the first methionine, we believe that the first 158 nt are part of the 5′ untranslated region (UTR) for the following two reasons. Firstly, although the first 52 amino acids are in frame with the first methionine, BLAST analyses with this region did not retrieve any similar sequences from publicly available databases. Secondly, using the *ScORK17* nucleotide sequence, a seed derived tomato (*Solanum lycopersicum*) EST (SGN-U342343) was found in the SOL Genomics Network database (http://www.sgn.cornell.edu/). This single EST aligned with the *ScORK17* 5′ end with 94% nucleotide sequence identity. Alignment of the translated product of SGN-U342343 with ScORK17 showed 95% amino acid sequence identity (98% similarity) starting from the first methionine found in each cDNA. Furthermore, in tomato, in frame stop codons were found upstream of the first methionine and the length of the 5′UTRs were comparable, 158 nt for ScORK17 and 130 nt for SGN-U342343. This data strongly suggests that methionine 53 starts the open reading frame of *ScORK17*. More in depth sequence analysis revealed that *ScORK17* encodes a receptor kinase of the LRR-VI family (Shiu and Bleecker 2003) and exhibits the typical structure of LRR-RLK: a predicted signal peptide (1–27), a transmembrane domain (394–416), a kinase domain (483–757), and a short C-terminal tail (758–778) (Fig. 1a). A more exhaustive analysis of the extracellular domain revealed that it contained ten predicted leucine-rich repeats (LRR) located between amino acids 110 and 341 (Fig. 1a, b) (Obenauer et al. 2003). Two cysteine pairs flank these LRRs. The N-terminal cysteine pair (CNSEPNTALTLMC) is located 60 amino acids from the start codon and is very similar to the cysteine pair (CNSEPSPSLTVVC) in the closest *Arabidopsis* ortholog (At3g03770, see also below for phylogenetic analysis). The C-terminal cysteine pair (CLSNKEQWQHPYSFC) is located 14 amino acids downstream of the last LRR (LRR10). Seven N-glycosylation sites are also predicted from the ectodomain sequence (Gupta and Brunak 2002). Analysis of the kinase catalytic domain revealed that ScORK17 could be classified as an ACF kinase (alternative catalytic function). In *Arabidopsis*, these kinases comprises 20% of the *Arabidopsis* kinome and their catalytic domain lack one or more of three highly conserved residues (K/D/D) thought to be required for catalytic activity in subdomains II (K), VI (D), and VII (D) (Dardick and Ronald 2006). Analysis of all LRR-VI kinases in both *Arabidopsis* and rice revealed that they all belong to the ACF kinase group (Shiu et al. 2004).

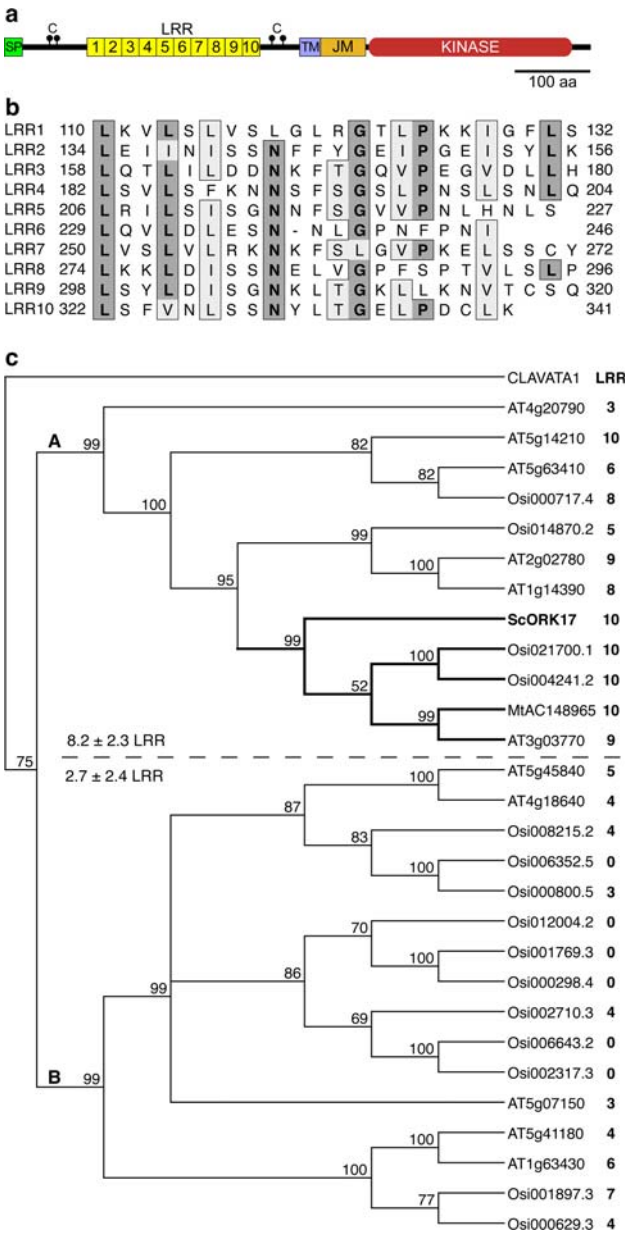

Fig. 1 **a** Illustration of ScORK17 primary structure. *Dots* correspond to the cysteine pairs. *SP* signal peptide, *LRR* leucine-rich repeat, *TM* transmembrane domain, *JM* intracellular juxtamembrane domain, *KINASE* kinase catalytic domain. **b** The ten LRRs are aligned to emphasize most frequent amino acids found at regularly spaced positions. *Dark grey boxes* represent conserved residues in more than half the sequences while *light gray boxes* represents conservative substitutions. **c** A neighbour-joining clustering from the kinase domain of the ScORK17 receptor kinase and all the LRR-VI subfamily RLK members from *A. thaliana* and rice, as well as a highly similar RLK from *Medicago truncatula*. The kinase domain from the CLAVATA1 RLK from the LRR-XI subfamily was chosen as the outgroup. Bootstrap values were calculated from 10,000 replicas. The branch corresponding to the ScORK17 most probable orthologs is highlighted in *bold*. *Numbers* of LRR predicted for each receptor kinase appear on the right of each accession number or gene name

BLASTP analysis revealed that ScORK17 shared 72% similarity (54% identity) with a *Medicago truncatula* RLK (ABD28527 or AC148965), 71% similarity (52% identity) with the At3g03770 *Arabidopsis* LRR-VI family RLK (Shiu and Bleecker 2003), and 66% similarity (46% identity) with a rice (*Oryza sativa*) LRR-VI family RLK (Osi021700.1) (Shiu et al. 2004). The second closest hit in *Arabidopsis*, At2g02780, shares strikingly less sequence similarity (54%), leaving At3g03770 as the most likely *Arabidopsis* ortholog for *ScORK17*. To better determine the closest orthologs in *Arabidopsis* and rice for *ScORK17,* a phylogenetic analysis was performed with all the LRR-VI family members and with the Clavata1 RLK from the LRR-XI family as the outgroup. Since these two organisms have been fully sequenced, LRR-VI family members have already been annotated (Shiu et al. 2004). Because in this family the LRRs are quite variable in numbers (from 3 to 10 in *Arabidopsis*, and from 0 to 10 in rice as predicted by Scansite 2.0) the phylogenetic analysis was performed with the kinase domains only, as used previously to determine their family grouping (Shiu et al. 2004). This explains why some LRR-VI family members in rice have no predicted LRR under high stringency. The phylogenetic analysis is shown in Fig. 1c. ScORK17 clusters with a highly supported group of four RLKs, including the ones retrieved from the BLASTP search as being the most similar. Using a motif prediction algorithm (Scansite 2.0) the number of LRRs present in each RLK was also determined under high stringency conditions (Fig. 1c). Although the phylogeny was based on the kinase domain only, ScORK17 clustered with RLKs also having the most numerous LRRs in their ectodomains, suggesting a tight functional constrain and, possibly, that this subgroup was already present before the divergence between eudicots and monocots. Interestingly, phylogenetic association between the kinase domains mostly reflected the LRR organization with RLKs possessing numerous LRRs (8–10) clustering together, while RLKs possessing fewer LRRs ($\leq$6) also clustering together in two separate highly supported branches (branches A and B on Fig. 1c). LRR-VI RLKs from branch A (8.2 ± 2.3 LRRs) have three-fold more LRRs than the ones on the B branch (2.7 ± 2.4 LRRs).

ScORK17 expression analysis and localization

ScORK17 mRNA expression was first assessed by RNA gel blot analysis using a variety of vegetative and reproductive tissues (Fig. 2a). In order to get a more detailed picture of *ScORK17* expression in the developing fruit, the structure was dissected in ovules plus placenta and pericarp separately. *ScORK17* mRNA expression was undetectable in non-female reproductive tissues, confirming previous results obtained by quantitative real-time PCR (Germain et al. 2005). In ovary tissues, *ScORK17* expression is also barely detectable before fertilization but increases strongly following fertilization, in full concordance with previous quantitative RT-PCR analyses. Peak accumulation occurs 4 days after pollination (96 HAP) which corresponds to ovules at the zygotic stage or two-cell proembryo (Fig. 2a, b, Lafleur E. and Matton D. P. unpublished observations). *ScORK17* mRNA accumulation decreases thereafter and reaches pre-fertilization levels by 16 DAP. *ScORK17* mRNA signal is detected both in ovules and placenta as well as in the fruit pericarp.

In order to determine more precisely the spatial expression pattern of *ScORK17*, in situ RNA hybridizations were performed using ovaries taken 4 days after pollination, when peak accumulation occurs (Fig. 2a). *S. chacoense* produces unitegmic-tenuinucellate ovules, a trait that occurs almost universally in the asterid clade (Albach et al. 2001). As for other solanaceous species, the nucellus is completely utilized during megagametophyte development (Dnyansagar and Cooper 1960; Lee and Cooper 1958; Souèges 1907). The embryo sac is thus in direct contact with the endothelium, also called the integumentary tapetum, a layer that is formed as the result of the transformation of the integumental epidermis into specific secretory cells on the nucellus side of the megagametophyte and that retains meristematic properties (Batygina 2002). The endothelium layer is easily recognized with its large isodiametric cells with clearly defined nucleus and dense cytoplasm (Fig. 2b, panels i and ii, red arrowheads). The remaining layers of the integument are mostly made of parenchymous cells. Immediately adjacent to the endothelium, the inner integumentary cells appear crushed, probably due to the expansion of the developing endosperm (Fig. 2b, panel ii, green arrowhead). This is consistent with what has been described in other solanaceous species (Dnyansagar and Cooper 1960; Lee and Cooper 1958; Sin et al. 2006).

As seen in Fig. 2b panels iii, v, and vii, strong *ScORK17* mRNA signal was detected in the single ovule integument that is developing into the seed coat. By this stage, *Solanum* ovule integument would have undergone a few rounds of cell division (Olson 1988; Sin et al. 2006). Also, ovules contain cellularized endosperm that can be seen as a large vacuolated area in the center (Fig. 2b panels i, ii, v, vii, viii). As observed through DIC microscopy (Fig. 2b panel ii), the cell layers just outside of the endothelium also appear crushed, and this is more prominently visible at the chalazal end of the ovule (Fig. 2b, panel viii). Interestingly, the strongest *ScORK17* mRNA signal was detected in the cell layer next to the crushed cells, forming a more densely stained ring (Fig. 2b, panels v, vii, and viii, yellow arrowhead), while the crushed cell layer was much less stained and appeared as a light blue ring around the endothelium (Fig. 2b, panels vii, viii, green arrowhead). There was also

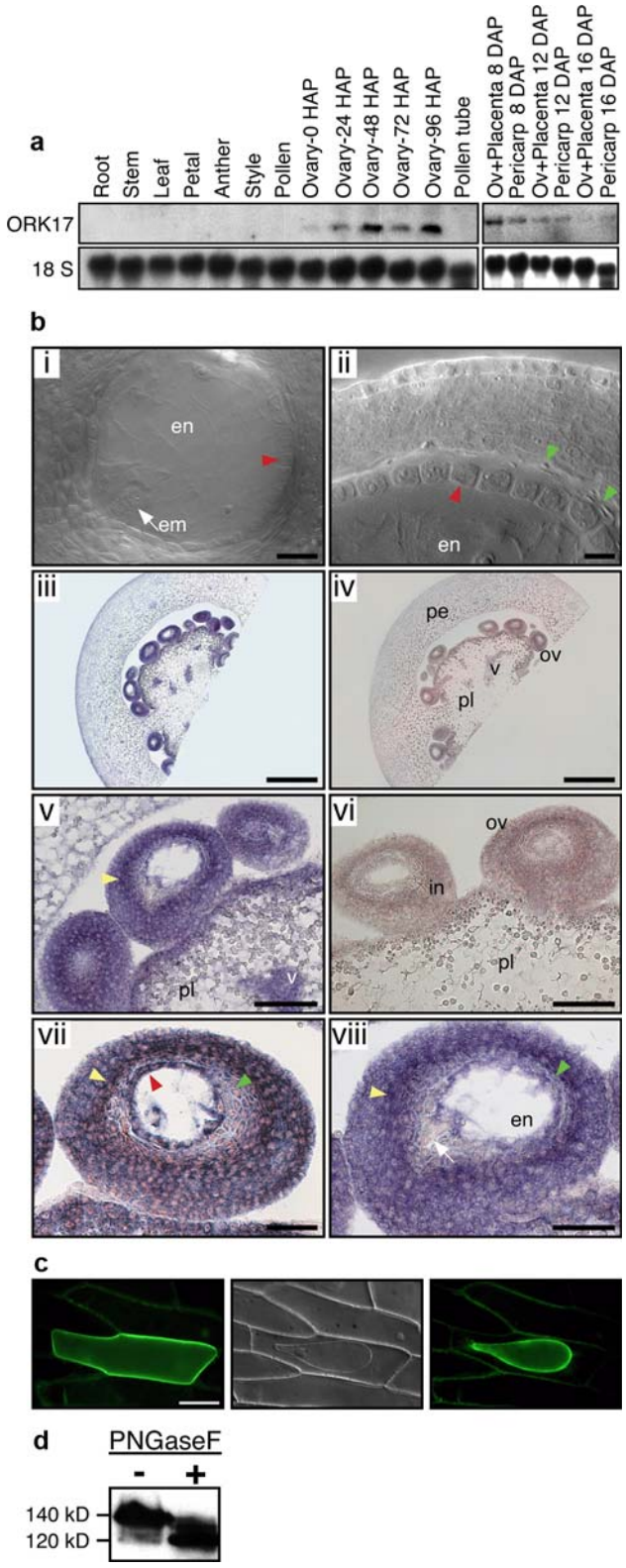

◀ **Fig. 2** Expression profile of *ScORK17*, subcellular localization and protein deglycosylation assay. **a** RNA gel blot analysis from vegetative and reproductive tissues. Equal loading of each sample was verified by ethidium bromide staining prior to gel transfer (not shown) and by 18S rRNA hybridization. For pollen tube RNA isolation, pollen was germinated on a solid media covered by a 0.45 µm nylon filter to facilitate pollen tube isolation. **b** In situ mRNA localization of *ScORK17* transcripts in fertilized ovaries (iii–viii). Ovaries were harvested 4 days after pollination and in situ hybridization was performed using either antisense (iii, v, vii, viii) or sense (iv, vi) probes from the *ScORK17* cDNA clone. Digoxigenin labeling is seen as *bluish purple* staining. Hybridizations were performed under identical conditions for both antisense and sense probes. Cleared ovule DIC images (i, ii) are also provided to better distinguish the cell layers organization. *Scale bars* 25 µm (i); 50 µm (vii, viii); 100 µm (ii, v, vi) and 500 µm (iii, iv). Abbreviations: *em* embryo, *en* endosperm, *in* integument, *ov* ovule, *pe* pericarp, *pl* placenta, *v* vasculature. *Arrowhead* indicates the endothelium layer. *Red arrowheads* indicate the endothelium layer surrounding the embryo sac; *green arrowheads* indicate the crushed layer of integument cells immediately surrounding the endothelium; *yellow arrowheads* indicate the hybridization dense cell layer surrounding the crushed cells layer; *white arrow* indicates the 2-celled proembryo at 4 DAP. **c** Plasma membrane localization of ScORK17. Epidermal onion cells expressing the ScORK17-GFP construct after microparticles bombardment and observed under fluorescent illumination before (*left panel*) and after plasmolysis (*right panel*). *Middle panel*: Differential interference contrast (DIC) microscopy of the same cells after plasmolysis showing protoplast shrinkage. **d** Deglycosylation assay from transiently expressed ScORK17 protein in *Nicotiana benthamiana* leaves through agroinfiltration. A ~ 20 kD gel shift is observed after treatment (+) with PNGase F (N-glycosidase F). (−) lane, sample without PNGase F treatment

an intense signal in the endothelium (Fig. 2 panel vii, red arrowhead). *ScORK17* mRNA signal was also present in the endosperm; however, due to large vacuoles in the cellular endosperm, it was not as strong as the one observed in the integument (Fig. 2b, panels vii, viii). Occasionally, an intense signal was observed around the endosperm nuclei (data not shown). In paraffin embedded sections where embryos could be identified, no clear *ScORK17* mRNA signal could be found (Fig. 2b, panel viii, white arrow). *ScORK17* mRNA signals were also detected in the placenta, mainly in the placental epidermis and in the placenta vasculature (Fig. 2b, panels iii, v), and light staining was consistently observed in the ovary pericarp. *ScORK17* sense probe hybridizations were performed as negative controls and gave no signal in pericarp, ovule, or placenta (Fig. 2b, panels iv, vi).

Although it is generally assumed that LRR-RLKs are localized at the plasma membrane, the subcellular localization of few LRR-RLKs has been investigated. To determine the subcellular localization of ScORK17, a fusion protein harboring a green fluorescent protein (GFP) downstream of the ScORK17 open reading frame (ORF) was constructed. Transient expression of ScORK17::GFP through particle bombardment of onion epidermal cells was performed. ScORK17 could be localized to the cell periphery in non-plasmolyzed cells (Fig. 2c, left panel). Plasmolysis was performed and a DIC image of the same cell layer shows the cell structures after plasmolysis, clearly showing the cell wall and the plasma membrane of the shrunken protoplasm (Fig. 2c, middle panel). In the plasmolyzed cell, the

fluorescent signal is unambiguously restricted to the plasma membrane and absent from the cell wall (Fig. 2c, right panel) thus clearly indicating that ScORK17 localizes at the plasma membrane.

Since several N-glycosylation sites were predicted from the primary amino acid sequence of ScORK17, a N-deglycosylation assay was performed to determine if ScORK17 is a N-glycosylated receptor kinase. The ScORK17 ORF fused to GFP was transiently expressed through agroinfiltration in *Nicotiana benthamiana* leaves and a crude protein extract was submitted to deglycosylation with N-glycosidase F (PNGase F). PNGase F cleaves between the innermost GlcNAc and asparagine residues of high mannose, hybrid, and complex oligosaccharides from N-linked glycoproteins. The predicted molecular weight of ScORK17 without its signal peptide is 82.7 kDa. The observed molecular weight of ScORK17 after deglycosylation was ~120 kDa (ScORK17 ~ 83 kD + GFP-6His tag ~ 30 kD) and it was observed at ~140 kDa before deglycosylation. This mobility shift of ~20 kDa is consistent with the presence of several potential N-glycosylation sites (AsnXaa[Ser/Thr]) found in the ScORK17 ectodomain at positions 76, 138, 189, 215, 225, 315, and 326. Of these, five are predicted by the NetNGly 1.0 server as strong candidates for N-linked glycosylation (positions 76, 138, 215, 315, and 326). Another potential site (position 23) was excluded since it is embedded in the putative signal peptide.

Transgenic plant analysis

In order to obtain information with regards to the function of *ScORK17* we generated *S. chacoense* transgenic plants using either the full-length *ScORK17* clone or a truncated construct in which the intracellular domain was deleted. This later construct was designed to act as a dominant negative form of ScORK17. We obtained plants that overexpressed the transgene from both constructs (RNA gel blot analyses, data not shown) and these plants were analyzed for phenotypical abnormalities. No obvious defects were observed when the *S. chacoense* plants were transformed with the *ScORK17 S. chacoense* clones. Given the fact that our constructs were under the control of the 35S promoter we hypothesized that, either the transgenes were undergoing a mechanism of post-transcriptional regulation to alleviate an unfavorable effect of the high *ScORK17* transcript levels, or that phenotypical defects were either absent or undetected. We had previously shown that the 35S promoter was highly active in leaf, anther and ovary tissues (Gray-Mitsumune et al. 2006; O'Brien et al. 2007).

However, when we transformed the full *ScORK17* construct in *A. thaliana*, we observed that siliques contained significantly fewer seeds (Fig. 3a). The mutant plants obtained from independent transformed lines had an average of 15.7 to 24.2 seeds per silique compared to an average of 52.3 seeds per silique in the wild type (Fig. 3a, b). We confirmed expression of the transgene in the mutant plants using semi-quantitative RT-PCR (Fig. 3c). The average number of seeds per silique in the mutant lines was 22.2 (SD = 6.2) compared to 52.3 (SD = 8.0) in the wild type. For all lines, a Student's *t* test was carried out to verify that the changes in seed number were significant. All *P* values obtained were below 0.001, indicating that the changes observed in seed set were highly significant (*P* values for NF8 = 3.72E-9, for NF9 = 5.97E-29, and for NE2 = 0.0008). We carried out a careful observation to detect whether the mutant siliques also contained aborted seeds but none was observed, suggesting that the defect appeared earlier during ovule development, precluding fertilization of the affected ovules. To ascertain this, cleared ovules from *Arabidopsis* lines expressing the *ScORK17* construct were observed by differential contrast microscopy (DIC) to determine if megasporogenesis or megagametogenesis was affected. In these lines, all ovules observed produced a megaspore mother cell (MMC) (Fig. 4a). After meiosis, only 57% of the observed ovules had a clearly identifiable functional megaspore (FM,

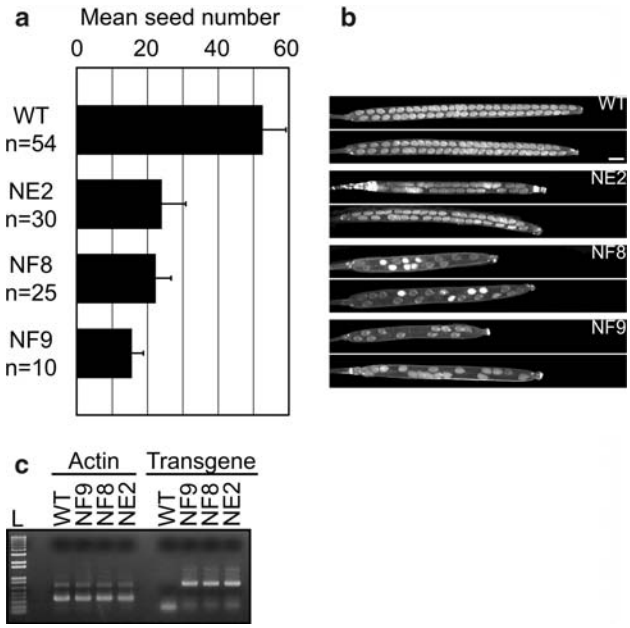

Fig. 3 Analysis of *Arabidopsis* transgenic lines expressing the *Solanum ScORK17* gene. **a** Seed count in wild type siliques versus siliques from three independent transformed lines (NE-2, NF-8, NF-9) overexpressing the full-length *ScORK17* construct. The number of siliques analyzed was $n = 54$ for *A. thaliana* WT Columbia ecotype. For the transgenic *A. thaliana* lines, $n = 30$ for the NE-2 line, $n = 25$ for the NF-8 line, and $n = 10$ for the NF-9 line. **b** Two examples of cleared siliques for each mutant line are shown. *Bar* equal 100 µm. **c** RT-PCR analysis of three independent transformed lines (NE-2, NF-8, NF-9) overexpressing the *ScORK17* construct. *L*, 1 kb DNA ladder

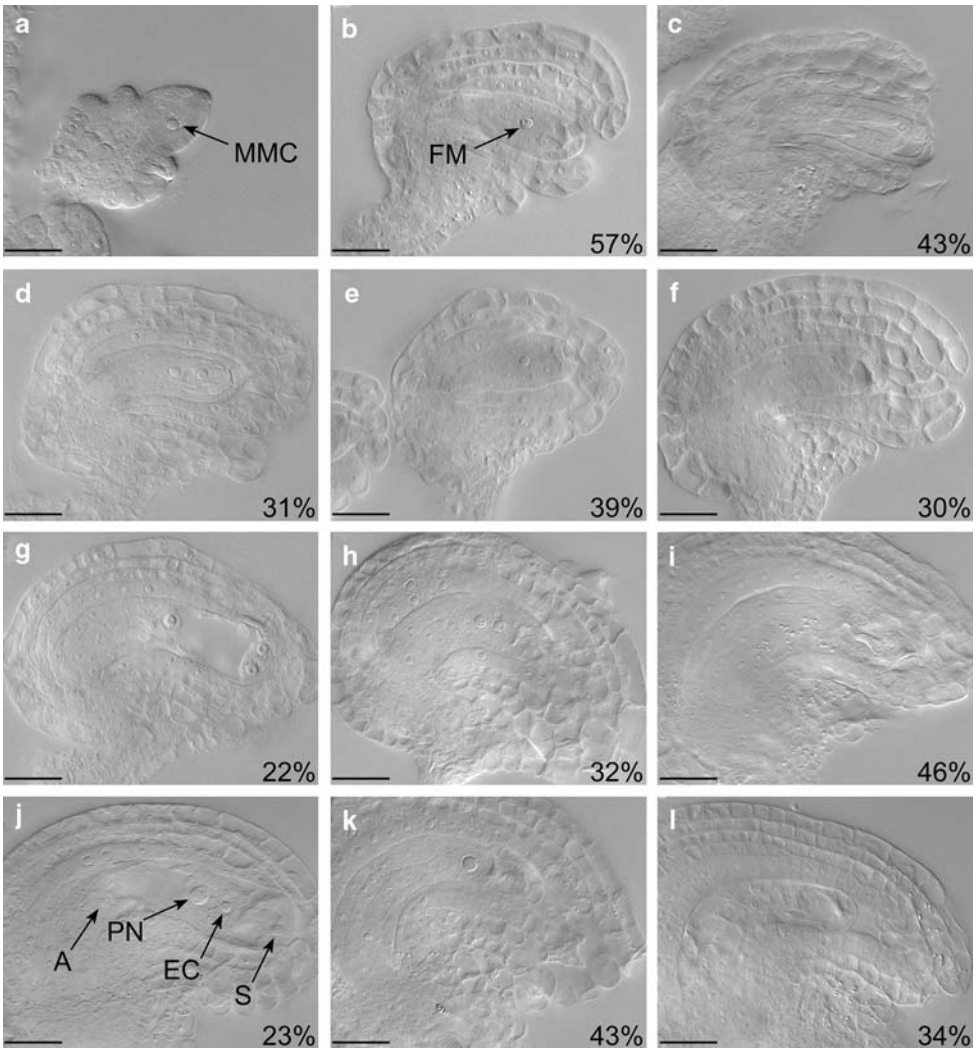

Fig. 4 Megasporogenesis and megagametogenesis in *A. thaliana* lines expressing the *ScORK17* construct. Cleared ovules were observed by DIC microscopy. Stages of embryo sac (ES) development as determined by floral bud length and ES cell number in WT Col. ovules and WT-looking ovules in the transformed lines. WT-looking ovules (**a**, **d**, **g**, **j**) from mutant lines. Ovules bearing abnormal ES from mutant lines (**b**, **c**, **e**, **f**, **h**, **i**, **k**, **l**). **a**–**c** functional megaspore stage. **d**–**f** binucleated megagametophyte. **g**–**h** tetranucleated megagametophyte. **j**–**l** octanucleated megagametophyte. *FM* functional megaspore, *A* Antipodals, *PN* Polar nuclei, *EC* egg cell, *S* synergid. *Scale bar* 20 μm

Fig. 4b). We then followed megagametogenesis and scored the ovule phenotypes as follows: WT-looking embryo sacs (Fig. 4b, d, g, j); aberrant embryo sac (ES), e.g., ES with less than the expected number of cells for the given stage (Fig. 4c, e, h, k); and absence of an ES when no cells could be observed in the ES (Fig. 4c, f, i, l). For all stages, a total of 100 cleared ovules were observed from the NF8 and NF9 lines. Percentage of wild type, aberrant or absent ES is indicated directly on the bottom right corner of the individual figures. At the functional megaspore (FM) stage, 43% of the ovules showed no visible FM in the region normally occupied by the ES. At the binucleate ES stage, 39% of the ovule ES had only one cell and 30% showed no visible cell. At the tetranucleate ES stage, 32% of the ovule ES had either 1 or 2 cells while 46% of the ovules showed no visible cell in the ES. Finally, at the mature ES stage (octanucleate), 43% of the ovule ES had either 1 or 2 cells while 34% of the ovules showed no visible cell in the ES. At this stage, ES with four cells were only rarely observed (<2%).

Discussion

Following fertilization, the embryo (and the fruit) starts to grow at a very rapid pace. This extremely active growth necessitates communication between the different structures of the fruit, including the embryo, the placenta, and the endosperm in order to maintain a synchronized and coordinated development. Biomolecules, most likely peptides, could mediate this communication through receptor kinases. To investigate the signal transduction events that take place during early embryogenesis in plants, we constructed a cDNA library enriched for weakly abundant RNA expressed in developing ovules (Germain et al. 2005). Despite the fact that receptor kinases have been associated with nearly all aspect of plant development, only few RLK have been associated with embryo development. We investigated the function of *ScORK17* since it presented an expression pattern highly specific to the early developing fruit following fertilization and was thus likely to be involved in fruit or embryo development.

Sequence analysis revealed that *ScORK17* is a member of the LRR-VI subfamily and displayed all the characteristics and domains found in plant receptor kinases. The phylogenetic analysis of all the LRR-VI members in rice and *Arabidopsis* highlighted the fact that two major clades are observed in the LRR-VI subfamily. This separation corresponds to the presence of a small or a large number of leucine-rich repeat although the phylogeny was performed with the kinase domain only. One clade had an average of 8.2 LRRs per protein while the other one had an average of 2.7 LRRs per protein (Fig. 1c). Shiu and Bleecker (2001) had previously observed that when the kinase domain of all the *Arabidopsis* receptor kinases was used to build a phylogenetic tree, members that had a similar extracellular domain type (LRR, S-domain, thaumatine-like, etc) tend to fall within the same clade. Grouping based on the structural arrangement of LRRs or on the location of introns in the extracellular domains of the individual RLKs was also observed (Shiu and Bleecker 2001). According to Shiu et al. (2004) the LRR-VI subfamily forms an ancestral unit, representing a clade (group) present before the monocot–dicot split (Shiu et al. 2004). Their analysis also led to the observation that genes involved in developmental processes are rarely found as tandem repeat in the genome whereas genes involved in resistance or defense response arose from duplication events which can be measured from a deviation to the 1:1 *Arabidopsis*–rice gene ratios (11 *Arabidopsis*: 15 rice in LRR-VI). Although nearly half of the LRR-VI *Arabidopsis* members are located on chromosome five none of them are found in tandem repeat (data not shown), hence supporting a developmental role for LRR-VI members and *ScORK17*.

RNA gel blot analysis (Fig. 2a) and quantitative RT-PCR results (Germain et al. 2005) have shown that *ScORK17* is almost exclusively expressed in female reproductive tissues, and is up-regulated following fertilization. A finer analysis using RNA in situ hybridization revealed that the *ScORK17* hybridization signal was strong in the ovule integument and in the endothelium, a layer that is formed as the result of the transformation of the integumental epidermis into specific secretory cells on the nucellus side of the megagametophyte (Batygina 2002). The endothelium has been proposed to serve multiple functions, mainly nutrient transport to the embryo sac and, in species where an endothelium persists in maturing seeds, like numerous species in the *Solanaceae*, a protective function toward the embryo and endosperm has also been proposed (Batygina 2002). Although no clear specialized cellular structures can be observed in the ovule single integument, strongest *ScORK17* mRNA signal was detected in the cell layer next to the crushed cells surrounding the endothelium, forming a densely stained ring (Fig. 2b, panels v, vii, viii), while the crushed cell layer was much less stained and appeared as a light blue ring around the endothelium (Fig. 2b, panels vii, viii). In *Solanum americanum*, Sin et al. (2006) described this layer as being gradually crushed by the pressure exerted by expanding endosperm, while Lee and Cooper (1958) considered that the inner integumentary cells immediately adjacent to the endothelium disintegrate. From our DIC pictures of cleared ovules, these cells appeared thin and elongated, as if they had been flattened, and large intercellular spaces between these cells were created, either the consequence of cellular flattening or due to a decreased number of cells, possibly explaining the weaker staining observed by in situ hybridization analysis. Weak *ScORK17* expression was also observed throughout the pericarp and in the placenta (Fig. 2b, panel iii). In the latter tissue, *ScORK17* expression was weak everywhere except in the vasculature and was as strong in the placental epidermis as in the ovule integument (Fig. 2b, panel v). Overall, the strong and very specific staining in ovules suggests that *ScORK17* plays a role in post-pollination ovule development. Contrary to the *ACR4* receptor kinase gene involved in epidermis tissues development in leaf and during ovule integument development (Gifford et al. 2003; Watanabe et al. 2004) and that is ubiquitously expressed in *Arabidopsis* (Tanaka et al. 2002), *ScORK17* displayed a more restricted expression pattern, mainly in the ovule integument and in the epidermal layer of the placenta. Strong mRNA expression in the placenta epidermal layer that is contiguous with the ovule integument, and ovular expression in layers derived from epidermal cells might suggest that the ScORK17 kinase is expressed in cells that express an epidermal cell fate but restricted to the female reproductive tissues.

Deglycosylation assay using transient expression in *Nicotiana benthamiana* leaves and PNGaseF treatment revealed that the predicted putative N-glycosylation sites were glycosylated in vivo. A large 20 kDa mobility shift observed after PNGaseF deglycosylation support the facts that several glycosylation sites are present. The presence of extensive glycosylation could also explain why our attempt to obtain a polyclonal antibody from rabbit immunized with an in vitro expressed extracellular domain (devoid of post-translational modifications) could not recognize the plant produced ScORK17 protein (data not shown).

In order to determine the function of *ScORK17* in planta, we generated overexpressing transgenic plants in *S. chacoense* and *A. thaliana*. Although we obtained plants that overexpressed the *ScORK17* transcript in *S. chacoense*, no phenotype other than wild type could be observed. However, when we transformed *A. thaliana* with the *ScORK17* construct, plants with severely reduced seed set were obtained, confirming that *ScORK17* has a role in ovule or seed development. A careful examination of the ovules in lines expressing the *ScORK17* construct revealed that the

embryo sac was affected (Fig. 4). When compared to WT plants, ovules in the *Arabidopsis* lines expressing *ScORK17* bore a significant percentage of abnormal embryo sac. The observed defect started during megasporogenesis since at the MMC stage, already 43% of the ovules were devoid of an embryo sac. Megagametogenesis was also affected and, at the mature octanucleate stage, only 23% of the ovules bore fully developed ES, in concordance with the number of seeds that could be found in the siliques of these mutant lines (Fig. 3a). Thus, at a given flower development stage, ES development was either retarded, giving a lesser number of WT-like ES or, ES cells had already undergone degeneration. Nevertheless, at the end of megagametogenesis, most of the ovules bore abnormal ES resulting in the significantly lower seed set observed. Although the expression pattern observed for the *ScORK17* gene suggested a more prominent role in post-pollination ovule/seed development in *S. chacoense*, heterologous expression of the *ScORK17* RLK gene in *Arabidopsis* revealed a role in pre-fertilization events, mainly in embryo sac development. This could be the result of the use of a generic promoter to drive the *ScORK17* gene (35S promoter). Alternatively, *ScORK17* might be active at very low levels in developing ES in *S. chacoense* also, but this weak expression might not have been detectable through RNA gel blot analysis or in situ RNA hybridization (Fig. 2a, b). Nonetheless, heterologous expression resulted in a visible phenotype only in ovules, consistent with the highly specific *ScORK17* expression pattern in female reproductive tissues in *S. chacoense*. Considering the *ScORK17* expression in the endothelium and the integument (Fig. 2b) one cannot exclude a feedback effect from the surrounding sporophytic tissue on the developing ES. Using a microarray approach, Johnston et al. (2007) have recently shown the strong influence of the ES, in this case the absence of an ES, on gene expression in the surrounding sporophytic tissues. In their study, they showed that numerous genes were up-regulated (sporophytic gain of expression) in mutants lacking an embryo sac, suggesting that a substantial portion of the sporophytic transcriptome involved in carpel and ovule development is under the indirect influence of the embryo sac (Johnston et al. 2007). A converse effect from the endothelium and the integument, where *ScORK17* is mostly expressed, on the ES could also be envisaged.

As for the absence of phenotype in *S. chacoense*, we hypothesized, as mentioned in Diener and Hirschi (2000), that the differences in DNA sequence between the foreign gene and the host might have circumvented the host gene-silencing mechanism, enabling the observation of a mutant phenotype in a heterologous species (Hirschi et al. 2000). No phenotype other than wild type was observed in the only insertional T-DNA mutant line available at the time (see "Materials and methods"), possibly due to gene redundancy since the RLK family LRR-VI contains several members (11) and a related member could take over the function of the *Arabidopsis* gene corresponding to *ScORK17*, although the second closest ortholog (At2g02780) shares strikingly less amino acid sequence similarity (54%) when compared to At3g03770 (71%). The phenotypical defect observed in *Arabidopsis* plants over-expressing *ScORK17* is thus likely to be caused by either one or a combination of the following mechanisms. One possibility is that the abundantly expressed ScORK17 acts in a dominant negative manner in *Arabidopsis* by dimerizing with a receptor kinase that is involved in a pathway responsible for ovule and seed formation. The abundant ScORK17 receptor could also enhance the signaling activity of a receptor kinase or pathway that negatively regulates ovule and seed and formation. Alternatively, one cannot exclude the possibility that inappropriate temporal expression and, therefore, the production of a neomorphic gain-of-function mutation activates a substrate not normally activated by this RLK. Nevertheless, it is noteworthy that, although a generic promoter was used (CaMV 35S), the only defect observed in *Arabidopsis* transgenic lines was in the ovule, where *ScORK17* is predominantly expressed in *S. chacoense*.

It is likely that we did not observe any phenotype in *S. chacoense* because the ScORK17 protein level could be strictly regulated and degradation of the supernumerary transcript and/or protein, or truncated protein in the case of the dominant negative construct would occur, through a silencing mechanism. This mechanism would have been avoided in *A. thaliana* due the difference in sequence homology between *A. thaliana* and *S. chacoense* (Diener and Hirschi 2000). Heterologous transformation from plant to yeast (Alemzadeh et al. 2006; Ali et al. 2006; Weig and Jakob 2000) or from one plant species to another is of common use in order to uncover phenotype when silencing mechanism precludes protein accumulation in the host species either in a transformed population (Fu et al. 2007; Hirschi 1999; Hirschi et al. 2000) or when silencing affects subsequent generation (Liu and Zhang 2004).

We presented evidences that *ScORK17*, coding for a plant receptor kinase of the LRR-VI subfamily, could be involved in plant reproductive development. *ScORK17*, whose expression is highly specific to the ovary and more precisely to the ovule integument, partially block seed formation when expressed in *Arabidopsis*, mainly through the formation of ovules defective in embryo sac formation. The results presented in this paper represent, to our knowledge, the first functional study for a RLK member of the LRR-VI subfamily.

Acknowledgments We thank Gabriel Téodorescu for plant care and maintenance. H. Germain was the recipient of Ph. D. fellowships from the Natural Sciences and Engineering Research Council of Canada (NSERC) and from the Fonds Québécois de la Recherche en Nature et Technologie (FQRNT). NSERC and the Canada Research Chair program are also acknowledged for their support (D.P. Matton).

References

Albach DC, Soltis PS, Soltis DE (2001) Patterns of embryological and biochemical evolution in the asterids [Review]. Syst Bot 26:242–262

Alemzadeh A, Fujie M, Usami S, Yoshizaki T, Oyama K, Kawabata T, Yamada T (2006) ZMVHA-B1, the gene for subunit B of vacuolar H+-ATPase from the eelgrass Zostera marina L. Is able to replace vma2 in a yeast null mutant. J Biosci Bioeng 102:390–395

Ali R, Zielinski RE, Berkowitz GA (2006) Expression of plant cyclic nucleotide-gated cation channels in yeast. J Exp Bot 57:125–138

Batygina TB (ed) (2002) Embryology of flowering plants: terminology and concepts. Science Publishers, Inc., Endfield

Becraft PW, Stinard PS, McCarty DR (1996) CRINKLY4: a TNFR-like receptor kinase involved in maize epidermal differentiation. Science 273:1406–1409

Bendtsen JD, Nielsen H, von Heijne G, Brunak S (2004) Improved prediction of signal peptides: SignalP 3.0. J Mol Biol 340:783–795

Canales C, Bhatt AM, Scott R, Dickinson H (2002) EXS, a putative LRR receptor kinase, regulates male germline cell number and tapetal identity and promotes seed development in *Arabidopsis*. Curr Biol 12:1718–1727

Chantha SC, Emerald BS, Matton DP (2006) Characterization of the plant Notchless homolog, a WD repeat protein involved in seed development. Plant Mol Biol 62:897–912

Chevalier D, Batoux M, Fulton L, Pfister K, Yadav RK, Schellenberg M, Schneitz K (2005) STRUBBELIG defines a receptor kinase-mediated signaling pathway regulating organ development in *Arabidopsis*. Proc Natl Acad Sci USA 102:9074–9079

Clark SE, Running MP, Meyerowitz EM (1993) CLAVATA1, a regulator of meristem and flower development in *Arabidopsis*. Development 119:397–418

Clark SE, Williams RW, Meyerowitz EM (1997) The CLAVATA1 gene encodes a putative receptor kinase that controls shoot and floral meristem size in Arabidopsis. Cell 89:575–585

Curtis MD, Grossniklaus U (2003) A gateway cloning vector set for high-throughput functional analysis of genes in planta. Plant Physiol 133:462–469

Dardick C, Ronald P (2006) Plant and animal pathogen recognition receptors signal through non-RD kinases. PLoS Pathog 2:e2

Diener A, Hirschi H (2000) Heterologous expression for dominant-like gene activity. Trends Plant Sci 5:10–11

Dnyansagar VR, Cooper DC (1960) Development of the seed of *Solanum Phureja*. Am J Bot 47:176–186

Escobar-Restrepo JM, Huck N, Kessler S, Gagliardini V, Gheyselinck J, Yang WC, Grossniklaus U (2007) The FERONIA receptor-like kinase mediates male–female interactions during pollen tube reception. Science 317:656–660

Fu D, Huang B, Xiao Y, Muthukrishnan S, Liang GH (2007) Overexpression of barley hva1 gene in creeping bentgrass for improving drought tolerance. Plant Cell Rep 26(4):467–477

Garcia-Maroto F, Ortega N, Lozano R, Carmona MJ (2000) Characterization of the potato MADS-box gene STMADS16 and expression analysis in tobacco transgenic plants. Plant Mol Biol 42:499–513

Germain H, Rudd S, Zotti C, Caron S, O'Brien M, Chantha SC, Lagace M, Major F, Matton DP (2005) A 6374 unigene set corresponding to low abundance transcripts expressed following fertilization in *Solanum chacoense* Bitt, and characterization of 30 receptor-like kinases. Plant Mol Biol 59:515–532

Gifford ML, Dean S, Ingram GC (2003) The *Arabidopsis ACR4* gene plays a role in cell layer organisation during ovule integument and sepal margin development. Development 130:4249–4258

Gomez-Gomez L, Boller T (2000) FLS2: an LRR receptor-like kinase involved in the perception of the bacterial elicitor flagellin in *Arabidopsis*. Mol Cell 5:1003–1011

Gray-Mitsumune M, O'Brien M, Bertrand C, Tebbji F, Nantel A, Matton DP (2006) Loss of ovule identity induced by overexpression of the fertilization-related kinase 2 (ScFRK2), a MAPKKK from *Solanum chacoense*. J Exp Bot 57:4171–4187

Gupta R, Brunak S (2002) Prediction of glycosylation across the human proteome and the correlation to protein function. Pacific Symposium on Biocomputing, pp 310–322

Hirschi KD (1999) Expression of *Arabidopsis* CAX1 in tobacco: altered calcium homeostasis and increased stress sensitivity. Plant Cell 11:2113–2122

Hirschi KD, Korenkov VD, Wilganowski NL, Wagner GJ (2000) Expression of *Arabidopsis* CAX2 in tobacco Altered metal accumulation and increased manganese tolerance. Plant Physiol 124:125–133

Johnston AJ, Meier P, Gheyselinck J, Wuest SE, Federer M, Schlagenhauf E, Becker JD, Grossniklaus U (2007) Genetic subtraction profiling identifies genes essential for *Arabidopsis* reproduction and reveals interaction between the female gametophyte and the maternal sporophyte. Genome Biol 8:R204

Krogh A, Larsson B, von Heijne G, Sonnhammer EL (2001) Predicting transmembrane protein topology with a hidden Markov model: application to complete genomes. J Mol Biol 305:567–580

Lee JH, Cooper DC (1958) Seed development following hybridization between diploid *Solanum* species from Mexico, Central and South America. Am J Bot 45:104–110

Li J, Chory J (1997) A putative leucine-rich repeat receptor kinase involved in brassinosteroid signal transduction. Cell 90:929–938

Liu Y, Zhang S (2004) Phosphorylation of 1-aminocyclopropane-1-carboxylic acid synthase by MPK6, a stress-responsive mitogen-activated protein kinase, induces ethylene biosynthesis in *Arabidopsis*. Plant Cell 16:3386–3399

Matsubayashi Y, Ogawa M, Morita A, Sakagami Y (2002) An LRR receptor kinase involved in perception of a peptide plant hormone, phytosulfokine. Science 296:1470–1472

Matton DP, Maes O, Laublin G, Xike Q, Bertrand C, Morse D, Cappadocia M (1997) Hypervariable domains of self-incompatibility RNases mediate allele-specific pollen recognition. Plant Cell 9:1757–1766

Nodine MD, Yadegari R, Tax FE (2007) RPK1 and TOAD2 are two receptor-like kinases redundantly required for *Arabidopsis* embryonic pattern formation. Dev Cell 12:943–956

O'Brien M, Bertrand C, Matton DP (2002) Characterization of a fertilization-induced and developmentally regulated plasma-membrane aquaporin expressed in reproductive tissues, in the wild potato *Solanum chacoense* Bitt. Planta 215:485–493

O'Brien M, Chantha SC, Rahier A, Matton DP (2005) Lipid signaling in plants. Cloning and expression analysis of the obtusifoliol 14alpha-demethylase from *Solanum chacoense* Bitt., a pollination- and fertilization-induced gene with both obtusifoliol and lanosterol demethylase activity. Plant Physiol 139:734–749

O'Brien M, Gray-Mitsumune M, Kapfer C, Bertrand C, Matton DP (2007) The ScFRK2 MAP kinase kinase kinase from *Solanum chacoense* affects pollen development and viability. Planta 225:1221–1231

Obenauer JC, Cantley LC, Yaffe MB (2003) Scansite 2.0: proteome-wide prediction of cell signaling interactions using short sequence motifs. Nucleic Acids Res 31:3635–3641

Olson AR (1988) Postpollination placental development of a diploid *Solanum tuberosum*. Can J Bot 66:1813–1817

Rosso MG, Li Y, Strizhov N, Reiss B, Dekker K, Weisshaar B (2003) An *Arabidopsis* thaliana T-DNA mutagenized population (GABI-Kat) for flanking sequence tag-based reverse genetics. Plant Mol Biol 53:247–259

Saitou N, Nei M (1987) The neighbor-joining method: a new method for reconstructing phylogenetic trees. Mol Biol Evol 4:406–425

Shiu SH, Bleecker AB (2001) Receptor-like kinases from *Arabidopsis* form a monophyletic gene family related to animal receptor kinases. Proc Natl Acad Sci USA 98:10763–10768

Shiu SH, Bleecker AB (2003) Expansion of the receptor-like kinase/Pelle gene family and receptor-like proteins in *Arabidopsis*. Plant Physiol 132:530–543

Shiu SH, Karlowski WM, Pan R, Tzeng YH, Mayer KF, Li WH (2004) Comparative analysis of the receptor-like kinase family in *Arabidopsis* and rice. Plant Cell 16:1220–1234

Sin SF, Yeung EC, Chye ML (2006) Downregulation of *Solanum americanum* genes encoding proteinase inhibitor II causes defective seed development. Plant J 45:58–70

Souèges R (1907) Développement et structure du tégument séminal chez les Solanacées. Ann Sci Nat Bot XII 6:1–124

Tanaka H, Watanabe M, Watanabe D, Tanaka T, Machida C, Machida Y (2002) *ACR4*, a putative receptor kinase gene of *Arabidopsis thaliana*, that is expressed in the outer cell layers of embryos and plants, is involved in proper embryogenesis. Plant Cell Physiol 43:419–428

Tanaka H, Watanabe M, Sasabe M, Hiroe T, Tanaka T, Tsukaya H, Ikezaki M, Machida C, Machida Y (2007) Novel receptor-like kinase *ALE2* controls shoot development by specifying epidermis in *Arabidopsis*. Development 134:1643–1652

Torii KU, Mitsukawa N, Oosumi T, Matsuura Y, Yokoyama R, Whittier RF, Komeda Y (1996) The *Arabidopsis ERECTA* gene encodes a putative receptor protein kinase with extracellular leucine-rich repeats. Plant Cell 8:735–746

Voinnet O, Rivas S, Mestre P, Baulcombe D (2003) An enhanced transient expression system in plants based on suppression of gene silencing by the p19 protein of tomato bushy stunt virus. Plant J 33:949–956

Watanabe M, Tanaka H, Watanabe D, Machida C, Machida Y (2004) The *ACR4* receptor-like kinase is required for surface formation of epidermis-related tissues in *Arabidopsis thaliana*. Plant J 39:298–308

Weig AR, Jakob C (2000) Functional identification of the glycerol permease activity of *Arabidopsis thaliana* NLM1 and NLM2 proteins by heterologous expression in Saccharomyces cerevisiae. FEBS Lett 481:293–298